

EFFECTS OF WAKEFIELDS ON THE MICROBUNCHING INSTABILITIES AT PAL-XFEL

Eun-San Kim*

Pohang Accelerator Laboratory, Pohang, KyungBuk, 790-784 KOREA

Abstract

High bunch compression in two bunch compressors is required to achieve a peak beam current of about 3.5 kA in PAL-XFEL. We investigated effects of longitudinal space charge wake and geometrical linac wake on microbunching instability for the PAL-XFEL in the design stage. We show that significant energy modulation can be generated by the space charge wake and can enhance the coherent synchrotron radiation microbunching in the compressors for the PAL-XFEL. In this paper, we evaluated the total gain of the microbunching in the 3.7 GeV PAL-XFEL accelerator system. The evaluation was obtained by performing analytical calculations of integral equation for coherent synchrotron radiation microbunching [1].

INTRODUCTION

Bunch compressors are designed to shorten the bunch length and thus to obtain the peak current that is necessary to drive an X-ray free-electron laser (FEL). Many numerical and theoretical investigations have shown that the bunch compressor is affected a microbunching instability driven by coherent synchrotron radiation (CSR) [2]. It was also shown that the microbunching instability could be amplified by both density and energy modulation in upstream beam of the bunch compressor. Saldin et al. showed that the longitudinal space charge (LSC) wake might be a main source in driving the microbunching instability in the TTF2 linac [3]. Huang et al. also investigated the effect of the LSC wake and the geometrical linac wake on the CSR microbunching in the LCLS [4].

Bunch compressions of two stage in the PAL-XFEL are being designed to get a peak current of about 3.5 kA. Fig. 1 shows layout for the 3.7 GeV PAL-XFEL. The purpose of this paper is to estimate magnitude of the microbunching in the PAL-XFEL that can be driven by the CSR in two bunch compressors, the LSC wake and geometrical wake in S-band linac. It is shown that the LSC wake may induce considerable energy modulation and enhance the CSR microbunching in the second bunch compressor of the PAL-XFEL.

MICROBUNCHING DUE TO CSR IN BUNCH COMPRESSORS

Momentum compaction factor R_{56} determines energy dependence of path length in a bunch compressor and the bunch can be compressed by $|1 + hR_{56}|^{-1}$, where h is

the energy slope. CSR emitted in a compressor can interact with the beam itself and increase the correlated energy spread. If the longitudinal density of the bunch is modulated at a short wavelength, CSR will induce energy modulation with the same wavelength. Such an energy modulation can be also transferred into density modulation in the bunch compressor.

In the presence of CSR, it was known that the bunching spectrum $b(k; s)$ was given by an integral equation [1]

$$b[k(s); s] = [b_o(k_o) - ik(s)R_{56}(s)p_o(k_o)]L(0, s) + ik(s) \int_0^s d\tau R_{56}(\tau \rightarrow s) \frac{I(\tau)}{\gamma I_A} Z[k(\tau); \tau] b[k(\tau); \tau] L(\tau, s), \quad (1)$$

where $b_o(k_o)$ and $p_o(k_o)$ are the initial density and energy spectra, respectively, $I(\tau)$ is the peak current at τ , I_A is the Alfvén current, $Z(k; s) = (1.63 + 0.94i)k^{1/3}/R^{2/3}$ is the steady-state CSR impedance for a bending radius $R(s)$, $L(\tau, s)$ denotes Landau damping from τ to s due to beam emittance and energy spread. The energy modulation spectrum is then given by [1]

$$p[k(s); s] = p_o(k_o)L(0, s) - \int_0^s d\tau \frac{I(\tau)}{\gamma I_A} Z[k(\tau), \tau] \times b[k(\tau), \tau] L(\tau, s). \quad (2)$$

The parameters for the bunch compressors are not determined, however a case of the bunch compressor parameters for our calculation is listed in Table I. The analytical solutions of Eqs. (1) and (2) are used to estimate the gain of density modulation due to the CSR in the bunch compressors of the PAL-XFEL. Fig. 2 shows the gain in density modulation as a function of wavelength at the exit of BC1. Fig. 3 shows the induced energy modulation $\Delta p_1(k_f; f)$ in units of initial bunching at the end of BC1. Fig. 4 shows the gain of density modulation at the exit of BC2 as a function of the wavelength. To estimate total gain due to the CSR in the BC1 and the BC2, we approximated the CSR energy kicks in BC1 as an effective energy modulation at the entrance of BC2 given by $\Delta p_2(k_o; 0) = E_1/E_2 \Delta p_1(k_f; f)$. We also assume that the density modulation in BC1 is maintained to the entrance of BC2. Fig. 5 shows total gain of the density modulation that is induced by both the density and the energy modulations in BC2.

MICROBUNCHING DUE TO LONGITUDINAL SPACE CHARGE

In this section, we investigate the effect of the LSC wake on the CSR microbunching in the bunch compressors. Longitudinal density modulation in a beam can induce beam

* eskim1@postech.ac.kr

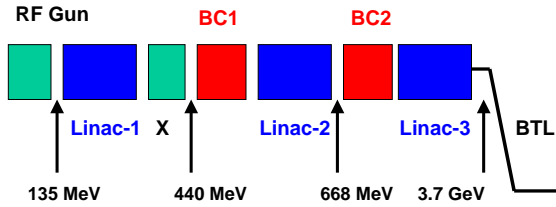


Figure 1: Layout of the PAL-XFEL accelerator system.

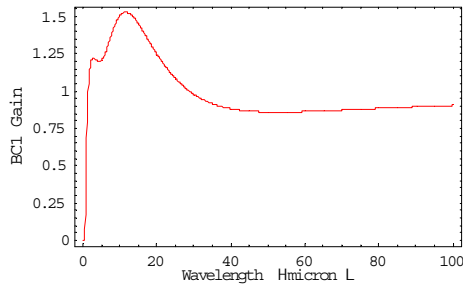


Figure 2: Gain of density modulation at exit of BC1.

energy modulation due to itself's space charge field in the linac. The generated energy modulation is then transferred to density modulation due to the R_{56} component in the bunch compressor.

The free-space LSC impedance per unit length is [5, 6]

$$Z_{LSC}(k) = \frac{iZ_o}{\pi k r_b^2} \left[1 - \frac{k r_b}{\gamma} K_1\left(\frac{k r_b}{\gamma}\right) \right], \quad (3)$$

where $Z_o = 377\Omega$ is the free space impedance, r_b is approximately taken as rms beam size, γ is the electron energy in units of its rest mass, K_1 is the modified Bessel function, $k = 2\pi/\lambda$ and λ is the modulation wavelength.

Beam energy is roughly 135 MeV at the end of the PAL-XFEL photoinjector and is accelerated up to 420 MeV in linac Linac-1. In the Linac-1, the electron density modula-

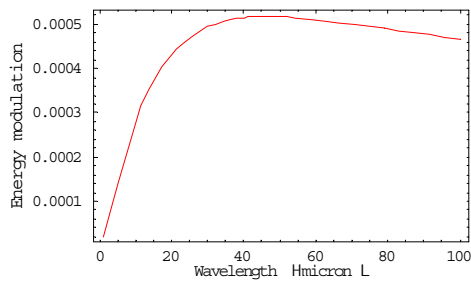


Figure 3: Gain of energy modulation at the exit of BC1.

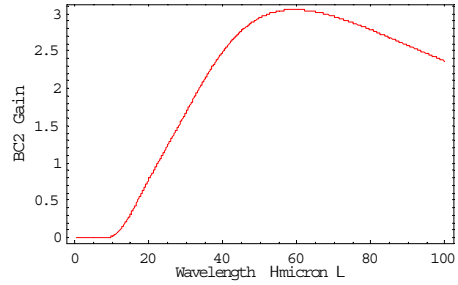


Figure 4: Gain of density modulation at the exit of BC2.

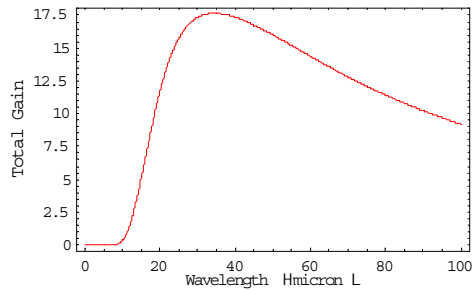


Figure 5: Gain of density modulation in both BC1 and BC2.

tion is frozen, but the energy modulation can be accumulated in the Linac-1. We investigate the gain due to small density modulations starting from the injector end. Uncorrelated energy spread at the BC1 is $\sigma_\delta = 7 \times 10^{-6}$. Figure 6 shows the gain of the density modulation at the exit of BC2 as a function of modulation wavelength at the entrance of BC2, including the LSC wake in the Linac-1 and Linac-2, and BC1. In result, it is shown that the peak gain in BC2 is significantly increased due to the LSC wake.

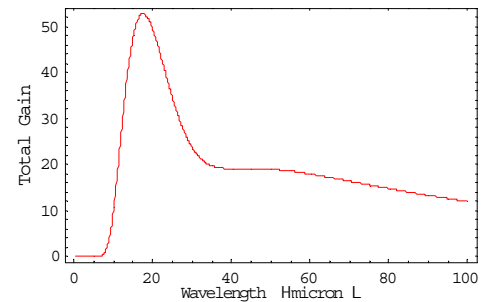


Figure 6: Gain of density modulation due to the LSC wake at the exit of BC2.

MICROBUNCHING DUE TO LINAC WAKE

In this section, we investigate the effect of linac wake on the CSR microbunching in the bunch compressors. Linac wake in upstream of a bunch compressor can generate energy modulation for a density-modulated beam and also induce additional density modulation in the bunch compressor. For an accelerating structure of S-band linac, the longitudinal impedance is given by [7]

$$Z_L(k) \approx \frac{4i}{ka^2} \left[1 + (1+i) \frac{\alpha L}{a} \left(\frac{\pi}{kg} \right)^{1/2} \right]^{-1}, \quad (4)$$

where a is the average iris radius, L is the cell length, g is the gap distance between irises and α is given by 0.5. Gain of density modulation in BC2 was calculated as a function of the initial modulation wavelength and the effect of the linac wake on the gain was shown to be negligible.

Table 1: Bunch compressor parameters that are used for our calculation.

Parameter	BC1	BC2
E(MeV)	429	668
I_f (A)	480	3500
ϵ_n (μm)	1	1
R_{56} (mm)	36	22
h (m^{-1})	-21.4	-40
L_b (m)	0.2	0.4
ΔL (m)	2.6	10
σ_δ	7×10^{-6}	2.78×10^{-5}

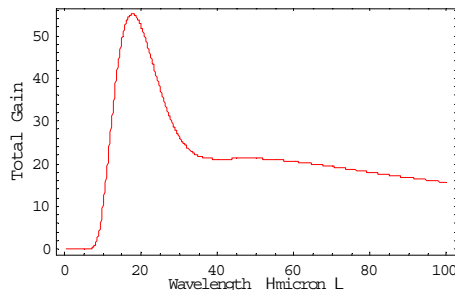


Figure 7: Total gain of the density modulation due to the LSC wake and the linac wake at the exit of BC2.

TOTAL GAIN IN PAL-XFEL

In this section we estimate the gain of the density modulation in the entire PAL accelerator by considering the CSR, the LSC wake and the linac wake. First, we calculate the induced density modulation in BC1 that is amplified by energy modulations from the LSC wake and the linac wake in Linac-1. For the given density modulation at the exit of

BC1, the LSC wake and linac wake in Linac-2 induce additional energy modulation. Finally we calculate in BC2 the final density modulation amplified from both density and energy modulations at the entrance of BC2. Fig. 7 shows the total gain as a function of the initial modulation wavelength due to LSC wake and the linac wake. Since $R_{56}=0$ in the BTL, the density modulation after BC2 remains the same. Then, we can roughly estimate the induced energy modulation by the linac impedance in Linac-3 and the CSR impedance in the BTL for the given b_f :

$$\Delta p_f \approx |I_f / \gamma_f I_A [Z_{Linac} L_{Linac-3} + Z_{CSR} L_{BTL}] b_f|, \quad (5)$$

where $L_{Linac-3} = 190\text{m}$ is the length of Linac-3 and $L_B = 10\text{m}$ is the total dipole length in the BTL. For the case of $\lambda_f = 20\ \mu\text{m}$, $I_f = 3.5\ \text{kA}$, $\gamma_f = 7400$ and the bending radius of the BTL dipoles $R = 56\ \text{m}$, final energy modulation Δp_f becomes $1.5 \times 10^{-5} b_f$. That means that b_f should be controlled less than 20 to satisfy with FEL parameter of $\rho = 4 \times 10^{-4}$ in the PAL-XFEL.

CONCLUSION

We have investigated the CSR microbunching instability that includes the effects of the LSC wake and linac wake in the PAL-XFEL. We have estimated the total gain of density modulation in the PAL-XFEL accelerator system. It was shown that the LSC wake can significantly increase the gain. This study suggests that we need to investigate to suppress the gain of the microbunching in the PAL-XFEL, including to find out an optimal location and compression factors of the BC1 and the BC2 as a future work.

We thank Z. Huang for useful discussions on the microbunching instabilities.

REFERENCES

- [1] Z. Huang, K.-J. Kim, Phys. Rev. ST Accel. Beams 5, 074401 (2002); Phys. Rev. ST Accel. Beams 5, 129903 (2002); Phys. Rev. ST Accel. Beams 7, 074401 (2004); Z. Huang et al., SLAC-PUB-9538 (2002).
- [2] S. Heifets, G. Stupakov, S. Krinsky, Phys. Rev. ST Accel. beams 5, 064401 (2002); E. L. Saldin, E. A. Schneidmiller and M. V. Yurkov, Nucl. Instrum. Methods Phys. Res., Sect. A 490 1 (2002).
- [3] E. L. Saldin, E. A. Schneidmiller and M. V. Yurkov, DESY Report No. TESLA-FEL-2003-02, 2003.
- [4] Z. Huang and T. Shaftein, in Proceedings of the 2003 Free-Electron Laser Conference, Tsukuba, Japan, 2003 (SLAC Report No. SLAC-PUB-9788, 2003). Z. Huang et al., Proc. of EPAC2004, Lucerne, 2206 (2004).
- [5] Z. Huang, M. Borland, P. Emma, K.-J. Kim, in Proc. of PAC2003, 3138 (2003).
- [6] J. Rosenzweig, C. Pellegrini, L. Serafini, C. Terzienden, and G. Travish, DESY Report No. TESLA-FEL-96-15, 1996.
- [7] R. L. Glckstern, Phys. Rev. D 39, 2780 (1989).